Allosteric Models for Multimeric Proteins: Oxygen-Linked Effector Binding in Hemocyanin†

Michael A. Menze,*,‡ Nadja Hellmann,§ Heinz Decker,§ and Manfred K. Grieshaber‡

Institut für Zoophysiologie, Heinrich-Heine Universität, Universitätsstrasse 1, 40225 Düsseldorf, Germany, and Institut für Molekulare Biophysik, Johannes-Gutenberg Universität, Jakob-Welder Weg 26, 55128 Mainz, Germany

Received March 20, 2005; Revised Manuscript Received June 13, 2005

ABSTRACT: In many crustaceans, changing concentrations of several low molecular weight compounds modulates hemocyanin oxygen binding, resulting in lower or higher oxygen affinities of the pigment. The nonphysiological effector caffeine and the physiological modulator urate, the latter accumulating in the hemolymph of the lobster *Homarus vulgaris* during hypoxia, increase hemocyanin oxygen affinity and decrease cooperativity of oxygen binding. To derive a model that describes the mechanism of allosteric interaction between hemocyanin and oxygen in the presence of urate or caffeine, studies of oxygen, urate, and caffeine binding to hemocyanin were performed. Exposure of lobster hemocyanin to various pH values between 7.25 and 8.15 resulted in a decrease of p50. In this pH interval, p50 decreases from 95 to 11 Torr without effectors and from 49 to 6 Torr and from 34 to 5 Torr in the presence of 1 mM urate or caffeine, respectively. Thus, the allosteric effects induced by protons and urate or caffeine are coupled. In contrast, isothermal titration calorimetry did not reveal any differences in binding enthalpy ($\Delta H°$) for urate or caffeine under either normoxic or hypoxic conditions at different pH values. Despite these apparently conflicting results, they can be explained by the nested MWC model if two different types of modulator binding sites are assumed, an allosteric and a nonallosteric type of site. Simulations of *in vivo* conditions with this model indicate that the naturally occurring modulator urate is physiologically relevant in *H. vulgaris* only during hypoxic conditions, i.e., either during environmental oxygen limitation or extensive exercise.

Hemocyanins are respiratory proteins found in the hemolymph of many species of the two phyla Mollusca and Arthropoda. The hemocyanins of many crustacean species are either hexamers or dodecamers with apparent molecular masses from 0.45×10^6 to 0.9×10^6 Da (*1*−*4*). The oxygen binding of crustacean hemocyanins, which first is characterized by the intrinsic properties of the protein, is modulated in addition by a number of inorganic ions and organic compounds of low molecular weight (*5*). Divalent cations (*6*, *7*), chloride (*8*), thiosulfate (*9*, *10*), neurohormones such as dopamine or octopamine (*11*, *12*), and anaerobic end-products such as L-lactate (*13*, *14*) and urate (*15*−*17*) are modulators of hemocyanin function.

Morris et al. (*17*) were able to show that urate increases hemocyanin oxygen affinity in the freshwater crayfish *Austropotamobius pallipes*, and the urate effect was confirmed later for several other species (*5*). Hemolymph urate concentrations were found to accumulate in response to environmental hypoxia and/or to a lesser extent during extensive exercise (*18*, *19*), because urate cannot be further metabolized anaerobically to hypoxanthine if uricase (urate oxidase; EC 1.7.3.3) lacks its second substrate oxygen (*18*). Thus, urate must be considered a physiological modulator of hemocyanin oxygen affinity in several crustaceans. In addition, the urate analogue caffeine as well as other purine derivatives were described as effectors of oxygen affinity, with some of them being even more potent than urate (*20*). Purine derivatives such as caffeine can serve as useful model compounds, although they have no physiological relevance for the animal.

The hemocyanin of *Homarus vulgaris* is characterized by a strong Bohr effect that can be modulated by changing concentrations of urate. The decrease of p50 induced by urate is considerable and was shown to be pH-dependent (*15*, *16*). Despite the availability of these data, the oxygen-binding properties of hemocyanin from *H. vulgaris* have not yet been analyzed in terms of an allosteric model. For a number of other arthropod hemocyanin, concerted models such as the MWC model, the three-state MWC model or the nested MWC model were successfully employed to describe the oxygen-binding properties under different modulator concentrations such as protons, Tris, glycine, or dyes (*21*−*27*). A critical test of the validity of these models is to include modulator-binding affinities in the analysis. This has not been achieved so far for any crustacean hemocyanin but has recently been completed for the hemocyanin of the arachnid *Eurypelma californicum* (*28*).

† This work was supported by Deutsche Forschungsgemeinschaft (Gr 456/20-1), the State of Nordrhein-Westfalen (to M.K.G.) and the Naturwissenschaftlich-Medizinisches-Forschungszen-trum of the Johannes-Gutenberg University of Mainz (to H.D.).

* To whom correspondence should be addressed: Department of Biological Sciences, Louisiana State University, 202 Life Sciences Bldg., Baton Rouge, LA, 70803. Telephone: 225-578-1552. Fax: 225-578-2597. E-mail: menze@lsu.edu.

‡ Heinrich-Heine Universität Düsseldorf.

§ Johannes-Gutenberg Universität Mainz.

10.1021/bi050507s CCC: $30.25
Published on Web 07/09/2005

To understand the mechanism of allosteric interactions between the binding of oxygen and that of urate and caffeine to hemocyanin from *H. vulgaris*, oxygen-binding curves were determined in the absence and presence of both compounds as previously described (*29*, *30*). Furthermore, binding of both purines was measured under hypoxic conditions using isothermal titration calorimetry (ITC)[1] and compared to the results obtained previously for *H. vulgaris* under normoxic conditions (*31*). The experiments were performed at different pH values to address the allosteric coupling between protons and the two purines in hemocyanin of *H. vulgaris*. Allosteric models are applied to describe the interaction between protons, urate/caffeine, and oxygen and used to draw conclusions about the physiological relevance of urate as a natural modulator of hemocyanin oxygen binding in *H. vulgaris* under various conditions.

MATERIALS AND METHODS

Purification of Hemocyanin and Control of the Aggregation State. Purification and characterization of hemocyanin from the European lobster *H. vulgaris* was performed as described previously with regard to its molecular weight and aggregation state (*31*).

ITC. All calorimetric experiments were performed with a VP-ITC titration calorimeter (MicroCal. Inc., Northampton, MA). Design and operation of the instrument was described previously (*32*). Protein solutions were prepared by dialysis of purified hemocyanin at 4 °C against 100 mM HEPES buffer (containing 20 mM $CaCl_2$, 20 mM $MgCl_2$, and 150 mM NaCl) adjusted to pH values as desired for the experiments. Ligand solutions were prepared by dissolving urate or caffeine in this buffer. Urate concentrations were checked spectrophotometrically using an extinction coefficient of $E_{293} = 12.6\ cm^2\ \mu mol^{-1}$ (*33*). Titration experiments were performed at 20 °C. The injection syringe rotated at 310 rpm, and the time interval between injections was about 400 s. The heat change accompanying the addition of buffer to hemocyanin and the heat of dilution of the ligands were subtracted from the raw data after correction for the injection signal of buffer into buffer. Titration curves were analyzed using Origin software (MicroCal. Inc., Northampton, MA). A "multiple noninteracting sites" model or "multisite interacting" model was used to analyze the data.

Modulator Binding Under Hypoxic Conditions. For measurement of the binding properties of urate and caffeine under hypoxic conditions, the VP-ITC titration calorimeter was transferred into a sealed experimental tent (Glovebag, Roth, Kalsruhe, Germany). During the experiment, the tent was continuously flushed with nitrogen. The sample cell of the VP-ITC was flushed with nitrogen for at least 1.5 h prior to the experiment. The ligand and the hemocyanin solution was equilibrated with humidified nitrogen at 17 °C using a tonometer and transferred into the experimental chamber using gas impermeable syringes (Hamilton, Reno, NV) flushed with nitrogen. Both solutions were degassed in the experimental tent with a vacuum degasser (ThermoVac, MicroCal Inc., Northampton, MA) for 30 min. The oxygen concentration in the experimental tent was continuously followed with an oxygen electrode (GMH 3691, Greisinger, Regenstauf, Germany). During the titration experiment, the oxygen concentration in the tent was less than 0.1% ($pO_2 <$ 1 Torr). As a control, a de-oxygenated and re-oxygenated hemocyanin sample was titrated with caffeine under normoxic conditions. The same slightly cooperative binding curve was obtained as with untreated hemocyanin, indicating that the de-oxygenation procedure did not lead to significant distortions of the protein. Furthermore, oxygen-binding curves of re-oxygenated hemocyanin agreed well with those of untreated samples.

Oxygen-Binding Studies. Hemocyanin oxygen equilibrium curves were obtained spectrophotometrically using a diffusion chamber method (*29*, *30*). With this method, oxygen tensions in the sample were varied at a set $P_{CO_2} = 0$, using gas mixing pumps (300 a/f, Wösthoff, Bochum, Germany). A total of 10−20 μL of a 20−30 μM solution of dodecameric hemocyanin was inserted into the light path of a photometer (photometer 1101 M, Eppendorf, Köln). The sample was equilibrated with a humidified gas mixture containing variable amounts of nitrogen, oxygen, and dehumidified CO_2 free air. The oxygen saturation of the pigment was determined by relating the absorbance ($\lambda = 365$ nm) of the sample at different oxygen concentrations to the difference in absorbance of completely oxygenated and deoxygenated hemocyanin. Oxygen-binding isotherms were measured at various pH values and in the presence or absence of 1 mM urate or caffeine as indicated in the captions of the figures and tables. Samples containing the modulators were prepared by adding a small volume of a concentrated stock solution of hemocyanin to the final sample.

Chemicals. Chemicals were purchased from Merck, Darmstadt, Roth, Kalsruhe, and Sigma, Deisenhofen, Germany.

THEORETICAL BASIS

Oxygen Binding. Oxygen-binding data were analyzed based on the three-state MWC model or the nested MWC model (*34*, *35*). For each model, the relevant binding polynomial P, as given below, was used to derive the function describing the saturation level θ by logarithmic differentiation with respect to the oxygen concentration x (eq 1). In the function finally applied to the data (θ_{fit}), minor uncertainties in the initial and final saturation level were allowed by introducing the parameters F_{fin} (for the final saturation level) and F_{in} (for the initial saturation level) for each binding curve individually

$$\theta_{fit} = (F_{fin} - F_{in})\theta + F_{in}$$

$$\theta = \frac{\partial \ln P}{n \partial \ln x} \quad (1)$$

In the ideal case, $F_{in} = 0$ and $F_{fin} = 1$, but because of experimental uncertainties, they were allowed to deviate by up to 3% from these ideal values.

Three-State MWC Model. The three-state MWC model is characterized by three different conformations that can be adopted by the allosteric unit (*34*). The allosteric unit defines a group of n monomers of an oligomer that are always in the same conformation under a specified set of conditions (*36*). Thus, for the 2× hexamer of hemocyanin from

[1] Abbreviations: ITC, isothermal titration calorimetry; [Hc], concentration of dodecameric haemocyanin; HEPES, *N*-[2-hydroxyethyl]-piperazine-*N*′-[2-ethanesulfonic acid]; TRIS, tris[hydroxymethyl]-aminoethane; p50, oxygen tension at half saturation.

H. vulgaris, $n = 6$ or 12 were used. These conformations are in equilibrium with each other as given by the corresponding allosteric equilibrium constants

$$L_T = \frac{[T_o]}{[R_o]} \qquad L_S = \frac{[S_o]}{[R_o]}$$

where $[T_o]$, $[S_o]$, and $[R_o]$ refer to the concentrations of unliganded (no oxygen bound) allosteric units in the respective conformation. Each conformation is characterized by its specific affinity for oxygen (K_S, K_R, and K_T). The binding polynomial is given by the following equation with $x =$ oxygen partial pressure pO_2

$$P = P_R^n + L_S P_S^n + L_T P_T^n$$
$$P_\alpha = 1 + K_\alpha x \quad \alpha = R, S, T \tag{2}$$

The allosteric equilibrium constants L_S and L_T depend on the modulator concentration. Thus, for each pH value and concentration of urate or caffeine, a specific value for L_S and L_T has to be allowed. The influence of urate on the values for L_S and L_T at any given pH value can be expressed as follows

$$L_{T,u} = L_T W_{T,u} \qquad L_{S,u} = L_S W_{S,u}$$
$$W_{T,u} = \frac{(1 + u_T[u])^m}{(1 + u_R[u])^m} \qquad W_{S,u} = \frac{(1 + u_S[u])^m}{(1 + u_R[u])^m} \tag{3}$$

Here, [u] is the free urate concentration, and u_R, u_T, and u_S are the urate-binding constants of the three conformations. The factors $W_{S,u}$ and $W_{T,u}$, as presented here, correspond to the simplest modulator binding model, where m identical binding sites per allosteric unit exists. For caffeine, the same kind of expression applies with the corresponding binding constants for caffeine (c_R, c_S, and c_T), and [c] is the free caffeine concentration. For the data analysis, subsets of data were analyzed simultaneously, using the factors describing the shift of the allosteric equilibrium constants as free parameters ($W_{T,u}$ and $W_{R,u}$, $W_{T,c}$ and $W_{R,c}$). These factors are independent of pH in the frame of the three-state model. The other parameters to be optimized are the oxygen-binding constants for each conformation (K_R, K_S, and K_T) and, for each pH value, two allosteric equilibrium constants [L_S(pH) and L_T(pH)] describing the conformational distribution in the absence of urate and caffeine.

Nested MWC Model. The general binding polynomial of the nested MWC model for a 2× hexamer of hemocyanin from *H. vulgaris* is given by (*35*)

$$P = (P_{rR}^6 + l_R P_{tR}^6)^2 + \Lambda(P_{rT}^6 + l_T P_{tT}^6)^2$$
$$\Lambda = L\frac{(1 + l_R)^2}{(1 + l_T)^2}$$
$$P_{\alpha\beta} = 1 + k_{\alpha\beta} x$$
$$\alpha\beta = tT, rT, rR, tR \tag{4}$$

Here, the existence of two levels of cooperativity is assumed, represented by two embedded allosteric units, a hexameric and dodecameric one. To simplify data analysis, the binding polynomial was written using the allosteric equilibrium constant Λ instead of L. The oxygen-binding constants for the four conformations are denoted by K_{tT}, K_{tR}, K_{rR}, and K_{rT}, and the equilibrium between the four conformations in the absence of oxygen is denoted by

$$L = \frac{[T]_o}{[R]_o} \quad l_T = \frac{[tT]_o}{[rT]_o} \quad l_R = \frac{[tR]_o}{[rR]_o} \quad \Lambda = \frac{[rT]_o^2}{[rR]_o^2}$$

The brackets denote the concentration of allosteric units in the different conformations [tT], [rT], [tR], and [rR] for the 6-meric allosteric unit and [T] and [R] for the 12-meric allosteric unit. Similar to the three-state MWC model, the influence of urate on the allosteric equilibrium constants at any given pH value can be expressed as

$$\Lambda_u = \Lambda F_u \qquad F_u = \frac{(1 + u_{rT}[u])^{2m}}{(1 + u_{rR}[u])^{2m}}$$
$$l_{T,u} = l_T F_{T,u} \qquad F_{T,u} = \frac{(1 + u_{tT}[u])^m}{(1 + u_{rT}[u])^m}$$
$$l_{R,u} = l_R F_{R,u} \qquad F_{R,u} = \frac{(1 + u_{tR}[u])^m}{(1 + u_{rR}[u])^m} \tag{5}$$

Again, the presentation of the factors F_u, $F_{T,u}$, and $F_{R,u}$ corresponds to the simplest possible modulator binding model with m identical binding sites per hexameric molecule. For caffeine, corresponding expressions were used.

Conformational Distribution. The conformational distribution (f_{tT}, f_{rT}, f_{rR}, and f_{tR}) of hemocyanin for the nested MWC model was calculated according to the following equations with P being the binding polynomial in eq 4

$$f_{tT} = \Lambda(P_{rT}^6 + l_T P_{tT}^6) l_T P_{tT}^6 / P$$
$$f_{rT} = \Lambda(P_{rT}^6 + l_T P_{tT}^6) P_{rT}^6 / P$$
$$f_{rR} = (P_{rR}^6 + l_R P_{tR}^6) P_{rR}^6 / P$$
$$f_{tR} = (P_{rR}^6 + l_R P_{tR}^6) l_R P_{tR}^6 / P$$

A feature in common with both models is that oxygen-binding data obtained under conditions such as different pH values or in the absence and presence of urate or caffeine are described by a common set of oxygen-binding constants. The influence of modulators is entirely reflected in the values of the allosteric equilibrium constants.

Fitting Strategy. As outlined above, the same set of three (three-state model) or four (nested MWC model) oxygen-binding constants are valid for all 12 oxygen-binding curves obtained under different conditions. Furthermore, for all curves obtained at a specific pH value (irrespective of the presence of urate or caffeine), common values for the allosteric equilibrium constants have to be assumed. The influence of the allosteric modulator urate and caffeine is incorporated with the factors F, F_T, F_R (nested MWC model), W_S, W_T (three-state MWC model; eqs 3 and 5). These factors are independent of the pH value in these models. The binding

curves were analyzed in subsets, where data at two pH values are clustered, each in the absence and presence of one of the modulators urate and caffeine. Thus, the oxygen-binding curves of a given subset were all linked through their common oxygen-binding constants and pair-wise linked through either common values for the allosteric equilibrium constants or the factors describing the shift in the allosteric equilibrium constants because of the presence of the modulator. Additionally, for each single oxygen-binding curve, two parameters allowing slight deviations with respect to the saturation level at 0 and infinite oxygen concentrations were introduced (eq 1). The fitting routine was set up to constrain these deviations to less than 3% from the ideal values ($F_{fin} = 1 \pm 0.03$ and $F_{in} = 0 \pm 0.03$).

The errors for the data sets were deduced from the variations among three oxygen-binding curves obtained at pH 8.0 in the absence of any modulator. The relative error in saturation dependent upon the saturation degree was calculated from the means and standard deviations of these three curves for a given oxygen concentration. A suitable function was fitted to this curve and used for the calculation of the typical errors for the other oxygen-binding curves, where only duplicates exist. These errors were used as weighting factors in the fitting routine applied to the subsets of oxygen-binding data.

To compare different types of models, the reduced χ^2 values were calculated based on the absolute errors (err) as deduced from the procedure mentioned above

$$\chi^2 = \frac{1}{DF}\sum\frac{(\theta_{meas} - \theta_{fit})^2}{err^2} \quad (6)$$

where θ_{meas} is the measured saturation degree, θ_{fit} is the value calculated from the fit, and DF is the degree of freedom (the number of data points minus the number of free parameters). Data were analyzed employing the Levenberg−Marquardt routine in SigmaPlot (SPSS Inc., Chicago, IL).

Analysis of Calorimetric Data. Binding of both urate and caffeine was analyzed based on two types of models. A model of interacting binding sites with two binding sites per 12-mer is based on the following binding saturation function with [e] being the modulator concentration (urate or caffeine) and [Hc] being the total hemocyanin concentration in dodecamers

$$[E_{bound}] = [Hc]\frac{K_1[e] + K_1K_2[e]^2}{1 + 2K_1[e] + K_1K_2[e]^2} \quad (7)$$

Binding to two types of binding sites is described by the following saturation function:

$$[E_{bound}] = [Hc]\left(\frac{2K_1[e]}{1 + K_1[e]} + \frac{2K_2[e]}{1 + K_2[e]}\right) \quad (8)$$

RESULTS

Oxygen-Binding Curves. Oxygen-binding curves were recorded at different pH values in the absence and presence of 1 mM urate or caffeine, yielding oxygen-binding curves for 12 different conditions. With increasing proton concentrations, the oxygen affinity of the pigment decreases from 11 Torr at pH 8.15 to 95 Torr at pH 7.25, confirming an already well-documented Bohr effect (*18*). Both purines increase the oxygen affinity of the pigment at any given pH value (Table 1). Furthermore, the Hill coefficient (n_H) is decreased in the presence of urate and caffeine, indicating a reduction in cooperativity (Table 1).

Table 1: Hill Parameters of Oxygen Binding to Hemocyanin from *H. vulgaris* at Different pH Values and in the Absence/Presence of 1 mM Urate or Caffeine[a]

pH	p50	p50 urate	p50 caffeine	n_H	n_H urate	n_H caffeine
8.15	11	6	5	3.7	2.9	2.6
8.00	13	8	6	4.0	3.3	3.0
7.85	17	10	7	4.3	3.5	3.0
7.55	34	20	14	4.4	3.7	3.2
7.25	95	49	34	3.8	3.5	3.1

[a] The values are the average of two measurements. Typically, the values differ by about 15%.

The simplest model for the description of cooperativity is the MWC model, which assumes two conformations, one prevailing under hypoxic conditions and the other prevailing under normoxic conditions. In a previous study, we have shown caffeine to bind cooperatively to oxygenated hemocyanin from *H. vulgaris* (*31*). This finding indicates that a third conformation relevant for the oxygenated state does exist. Therefore, a three-state MWC model (*34*) is the simplest model suitable for the description of allosteric regulation of this hemocyanin. To apply the model to the data, one would prefer to analyze all data sets simultaneously. This approach was impossible because the fitting routine allowed only a maximum of 25 parameters to be varied. Furthermore, it is useful to check the results of the analysis from different subsets for contradictions. Therefore, we fitted the corresponding saturation function (eq 1 and 2) to 4 subsets of the 12 data sets. These subsets were clustered as follows: (1) pH 7.55 ± urate, pH 8.15 ± urate; (2) pH 7.85 ± urate, pH 8.0 ± urate; (3) pH 7.55 ± caffeine, pH 8.15 ± caffeine; and (4) pH 7.85 ± caffeine, pH 8.0 ± caffeine.

An example of the results for one of the subsets (pH 7.55 + pH 8.15, ±urate) is shown in Figure 1. The fit of the three-state MWC model was performed based on either the hexamer or the 2× hexamer as an allosteric unit. On the basis of the reduced χ^2 values, it is not clear which variant delivers a better description (Table 2). However, when the size of the allosteric unit is free for optimization, the value tends to be closer to $n = 6$ than to $n = 12$. Therefore, only for $n = 6$, the values of the corresponding parameters are given. All oxygen-binding curves can be described well by one set of oxygen-binding constants: $K_R \geq 3$ Torr^{-1}, $K_S = 0.1 \pm 0.05$ Torr^{-1}, and $K_T = 0.004 \pm 0.003$ Torr^{-1}. The error estimates for the last two parameters are deduced from a fit, where K_R was set to 3 Torr^{-1}. This value represents a lower limit for K_R. It was defined as the value that leads to an increase of χ^2 by 2% compared to the value for χ^2 obtained when K_R was varied freely in the fitting routine, which yielded values with very high uncertainties because the upper limit is not well-defined. The final values for the allosteric equilibrium constants [L_T(pH) and L_S(pH)] and the factors W_S and W_T were obtained by setting the three oxygen-binding constants at fixed values. The agreement among the values for the allosteric equilibrium constants obtained from the

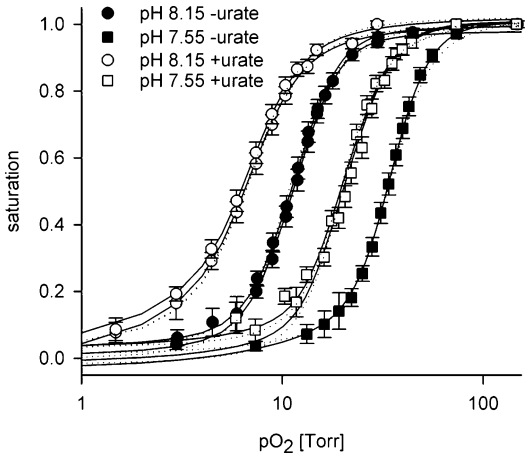

FIGURE 1: Oxygen-binding data. As an example, the oxygen-binding data obtained at pH 8.15 and 7.55 in the absence of any modulator (■ and ●) and in the presence of 1 mM urate are depicted. The lines correspond to the best fit based on the nested MWC model (···) or based on the three-state model (—). The values for half-saturation (p50) and the Hill coefficient for all oxygen-binding curves are summarized in Table 1.

Table 2: Comparison of Reduced χ^2

χ^2_{red}	pH 7.55 + 8.15 ±urate	pH 7.85 + 8.0 ±urate	pH 7.55 + 8.15 ±caffeine	pH 7.85 + 8.0 ±caffeine
three state, $n = 6$	1.2	0.4	0.6	1.2
three state, $n = 12$	0.4	1.5	0.6	1.0
nested MWC	0.5	0.4	0.4	0.8

different combinations of data is convincing (Figure 2a). Thus, the three-state MWC model seems to be a possible model for the allosteric regulation of this hemocyanin. On the basis of the values for the reduced χ^2 as shown in Table 2, one would not reject it, but it is not entirely satisfying.

It has been shown, that the nested MWC model is a suitable model for the allosteric regulation for a number of arthropodan hemocyanins (*7*, *21*, *24*, *25*, *27*, *37*, *38*). Thus, we also applied this model to the four subsets of oxygen-binding data. The strategy was essentially the same. The values for the four oxygen-binding curves were determined by a first analysis, where the values for the initial and final amplitude were not allowed to vary. Because this reduces the number of free parameters significantly, all data sets could be analyzed simultaneously. The affinity of conformation rT (K_{rT}) was not well-defined. Thus, the smallest possible value was determined in the same way as described for the three-state model, which yielded $K_{rT} = 3$ Torr^{-1}. Then, the oxygen-binding constants for the other conformations were $K_{rR} = 1.8 \pm 0.4$ Torr^{-1}, $K_{tR} = 0.065 \pm 0.004$ Torr^{-1}, and $K_{tT} = 0.008 \pm 0.0008$ Torr^{-1}. In the next step, the values for the oxygen-binding constants were set fixed to these values and the four subsets were analyzed in the same way as described for the three-state MWC model yielding now three allosteric equilibrium constants for each pH value [L_T(pH), L_R(pH), and Λ(pH)]. The oxygen-binding curves for the nested MWC model are also shown in Figure 1. The comparison of the reduced χ^2 values with those for the three-state MWC model is shown in Table 2, indicating overall a better agreement for the nested MWC model. The results for the allosteric equilibrium constants of the nested MWC model are shown in Figure 2b. For pH 8.25, 8.0, and 7.85,

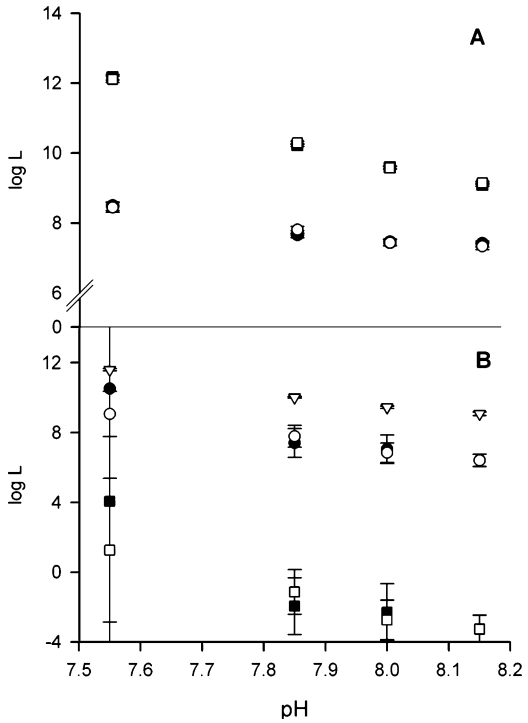

FIGURE 2: Allosteric equilibrium constants. Filled symbols indicate values obtained by subsets containing the curves in the presence of urate, and open symbols indicate those including caffeine. (A) Allosteric equilibrium constants as obtained from the four different subsets of oxygen-binding data are shown. The oxygen-binding constants were fixed in this analysis ($K_R = 3$ Torr^{-1}, $K_S = 0.1$ Torr^{-1}, and $K_T = 0.004$ Torr^{-1}), and the hexamer was assumed to be the allosteric unit. Squares correspond to L_T, and circles correspond to L_S. The factor describing the shift of the allosteric equilibrium constants were for urate $F_T = 0.036 \pm 0.006$ and $F_S = 0.39 \pm 0.07$ and for caffeine $F_T = 0.0066 \pm 0.001$ and $F_S = 0.22 \pm 0.05$. (B) Allosteric equilibrium constants of the nested MWC model. Triangles correspond to l_T, circles to l_R, and squares to Λ. The constants correspond to an analysis, where the value for the oxygen affinity to the conformation rT was set to the minimal value compatible with the data ($k_{rT} = 3$ Torr^{-1}). Then, the other three oxygen-binding constants are $k_{tT} = 0.008 \pm 0.0008$, $k_{rR} = 1.8 \pm 0.4$, and $k_{tR} = 0.065 \pm 0.004$ Torr^{-1}, and the allosteric equilibrium constants as shown in the figure. The factors describing the shift in allosteric equilibrium constants in the presence of urate or caffeine were for urate $F_{T,u} = 0.043 \pm 0.014$, $F_{R,u} = 0.056 \pm 0.006$, $F_u = 0.024 \pm 0.007$ and for caffeine $F_{T,c} = 0.0065 \pm 0.007$, $F_{R,c} = 0.024 \pm 0.0026$, $F_c = 0.015 \pm 0.005$.

the values obtained from the oxygen-binding curves in the presence of caffeine and urate agree well. For pH 7.55, the uncertainties are very large for both effectors, making a comparison difficult.

To obtain well-defined values for the factors F_R, F_T, and F (eq 5), the binding curves were reanalyzed based on a different clustering: all data curves in the presence of urate were analyzed simultaneously with fixed values for the oxygen-binding constants and the allosteric equilibrium constants. The same was performed with the oxygen-binding data in the presence of caffeine.

Calorimetric Data: Modulator Binding under Hypoxic Conditions. In this part of the study, binding of caffeine to hemocyanin from *H. vulgaris* under hypoxic conditions was investigated at different pH values. Because of the weak binding affinity of urate and the resulting experimental uncertainties, binding curves for this modulator were only measured at pH 7.55. Figure 3 shows a comparison of

Table 3: Thermodynamic Parameters for the Binding of Caffeine and Urate to Hemocyanin (*H. vulgaris*) under Hypoxic Conditions[a] Based on Two Effector Binding Sites Per Dodecamer

	caffeine				urate	
pH	K_1 (mM^{-1})	K_2 (mM^{-1})	ΔH_1° (kJ mol^{-1})	ΔH_2° (kJ mol^{-1})	K (mM^{-1})	ΔH° (kJ mol^{-1})
8.25	24.6 ± 2.7	27.9 ± 2.0	-106.8 ± 5.3	-71.5 ± 11.4	nd[b]	nd
8.15	12.6 ± 0.5	17.4 ± 3.2	-118.1 ± 18.9	-107.9 ± 11.5	nd	nd
8.00	18.6 ± 1.7	21.1 ± 3.8	$-113. \pm 11.6$	-75.0 ± 24.9	nd	nd
7.85	7.9 ± 3.0	13.4 ± 3.2	-111.9 ± 18.8	-87.5 ± 27.9	nd	nd
7.55	22.8 ± 4.1	12.4 ± 1.9	-91.1 ± 5.7	-126.9 ± 11.6	4.2 ± 0.580	-72.1 ± 8.2
7.25	10.7 ± 2.4	9.7 ± 1.6	-108.5 ± 6.0	-138.2 ± 25.8	nd	nd
$\bar{x}$	16.9 ± 6.0	17.0 ± 6.4	-108.4 ± 13.2	-103.0 ± 31.3	4.2 ± 0.580	-72.1 ± 8.2
normoxic[c]	14.5 ± 2.2	68.5 ± 10.7	-97 ± 16.0	-113 ± 10	8.5 ± 1.6	-135.0 ± 9.6

[a] Concentrations were 22.2−30.5 μM (12-mer). The concentration of the modulator solution was 1 mM. Experiments were performed at 20 °C. The errors given are the standard deviation of the mean (±SD). The errors given by the fitting routine for the individual parameters are in the same range. [b] nd = values not determined. [c] Values are from Menze et al. (*31*). The protein concentrations were 16.6−55.8 μM (12-mer). The concentration of the modulator solution was 0.6−2 mM. Experiments were performed at 20 °C. The errors given are the standard deviation of the mean (±SD). The errors given by the fit routine for the individual parameters are in the same range.

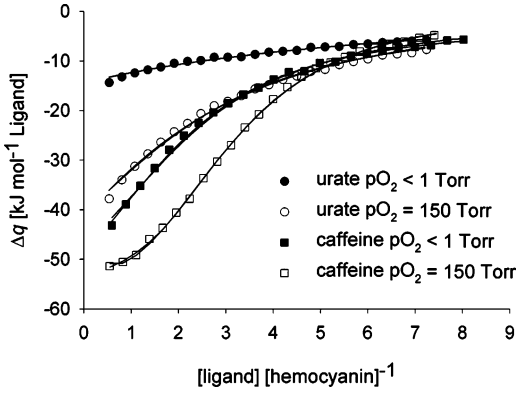

FIGURE 3: Titration of effector to hemocyanin (*H. vulgaris*) under hypoxic conditions. The titration experiments were performed at an oxygen concentration <1 Torr by injecting 24 × 10 μL of 1 mM urate (●) or caffeine (■) into hemocyanin (24−27 μM). All experiments were performed in HEPES buffer at pH 7.55 and 20 °C. For comparison, the curves obtained under normoxic condition (*31*) are shown (○, caffeine; □, urate). The lines correspond to the analysis based on (a) 2 identical binding sites per dodecamer (Table 3) and (b) 2 × 2 binding sites per dodecamer (Table 4). The curves based on the different types of analysis are practically identical (for details, see the text).

representative heat dissipation during isothermal titration of the two modulators under hypoxic (pO_2 < 1 Torr) and normoxic (pO_2 = 150 Torr) conditions at pH 7.55. Each point represents the heat Δq per mole of modulator liberated for an incremental addition of urate or caffeine, versus the ratio of the accumulated total modulator concentration divided by the concentration of hemocyanin.

The affinity of urate to hemocyanin under hypoxic conditions is not high enough to determine the binding stoichiometry accurately. The nonsigmoid shape of the binding curves does not provide enough information to determine all three parameters K, n, and ΔH°. In such a case, the number of binding sites is highly correlated with the binding enthalpy (*31*). Therefore, the same stoichiometry ($n = 2$ per dodecamer) as obtained under normoxic conditions was assumed in the analysis, yielding a good agreement between fit and data (Figure 3).

The two-interacting-sites model is the most general model assuming two binding sites. If the binding sites are not interacting, application of this model should yield similar affinities for the two binding steps. If heterogeneity or positive cooperativity is involved, distinctly different binding affinities will be obtained. Caffeine-binding data could formally be analyzed based on the "interacting sites" model. However, as shown in Table 3, the values for K_1 and K_2 do not differ significantly. Thus, binding of caffeine under hypoxic conditions can be described by a single binding constant of $K_1 \approx K_2 \approx 17$ mM^{-1}. For the same reasons, a single binding enthalpy $\Delta H^\circ \approx -106$ kJ mol^{-1} is obtained. Similarly, for urate, a binding constant of $K \approx 4$ mM^{-1} and a binding enthalpy of $\Delta H^\circ \approx -72$ kJ mol^{-1} has been determined (Table 3). Within the uncertainty of the parameters, no significant heterogeneity or positive cooperativity is observed. Surprisingly, no clear dependence of the binding affinity on the pH value can be seen (Table 3).

These data are in contrast to those obtained previously under normoxic conditions (*31*), which demonstrated that caffeine binds cooperatively ($K_1 \approx 14$ mM^{-1}, $K_2 \approx 40$ mM^{-1} and $\Delta H_1^\circ \approx -97$ kJ mol^{-1}, $\Delta H_2^\circ \approx -113$ kJ mol^{-1}), but also without any indications of a pH-dependent binding process (*31*). Urate was found to bind to hemocyanin noncooperatively also under normoxic conditions with a pH-independent affinity of $K \approx 8.5$ mM^{-1} and $\Delta H^\circ \approx -135$ kJ mol^{-1}. The comparison of the affinities reveals that the hemocyanin affinity for both effectors is reduced under hypoxic conditions compared to the affinity under normoxic conditions. This result is in agreement with the oxygen-binding data, which showed that urate and caffeine increase the mean affinity of hemocyanin, indicating a preferential binding of these modulators to the oxygenated species.

Model for Modulator Binding under Hypoxic and Normoxic Conditions. The nested MWC model was used to explain the results of the oxygen as well as modulator binding to hemocyanin. The shift of p50 in the presence of modulators to lower values is the result of a modulator-dependent change of the allosteric equilibrium constants, leading to a shift in the conformational distribution of the hemocyanin. The factors describing the shift in the allosteric equilibrium constants because of the presence of urate or caffeine contain the binding constants and stoichiometry of the corresponding modulators (eq 3 and 5). The results of the calorimetric data may be explained by the most simple model, which assumes $m = 1$ identical modulator binding sites per allosteric unit (the hexamer). Thus, for example, the factor $F_{T,u}$ for urate in the nested MWC model would be given by

Table 4: Thermodynamic Parameters for the Binding of Caffeine and Urate to Hemocyanin (*H. vulgaris*) under Normoxic and Hypoxic Conditions[a] Based on Four Effector Binding Sites per Dodecamer (Two Nonallosteric and Two Allosteric Urate/Caffeine-Binding Sites)

	urate			caffeine		
	K (mM^{-1})	$\Delta H°$ (kJ/mol)	$T\Delta S°$ (kJ/mol)	K (mM^{-1})	$\Delta H°$ (kJ/mol)	$T\Delta S°$ (kJ/mol)
nonallosteric deoxy	4	-61.9 ± 2	-41.7	33	-74.1 ± 0.6	-48.8
nonallosteric oxy	4	-70 ± 2	-49.8	33 ± 2	-47.4 ± 1	-22.1
conf. tT	0.5	-137 ± 12	-121	1.3	-83.1 ± 0.4	-65.7
conf. rT	34[$]	-53.3 ± 1	-27.9	361 ± 48	-56.1 ± 1	-25
conf. tR*	12			70		
conf. rR*	224			2960		

[a] Analysis was based on two types of sites per hexamer, where one site has an affinity independent of the conformation (nonallosteric). Results of the analysis for the four representative curves at pH 7.55 (Figure 3) are shown. The affinities for conformation rR and tR are based on the values for F_R, F_T, and F (see Figure 1) and the affinities for conformation rT. For details, see the text. $T\Delta S°$ was calculated based on $T\Delta S° = \Delta H° + RT \ln K$.

$F_{T,u} = [(1 + u_{tT})/(1 + u_{rT})]$, when the affinities u_{tT} and u_{rT} are given in mM^{-1}, because the modulator concentration was 1 mM in the oxygen-binding experiments. The values for u_{tT} and u_{rT} can be determined directly by calorimetric experiments if conditions are found where the conformations tT and rT dominate and are not changed significantly upon modulator binding. To check whether these conditions are met in the ITC experiments, the conformational distributions of hemocyanin at 1 and 150 Torr pO_2 were calculated for the four different pH values in the absence and presence of 1 mM modulator. For this modulator concentration, the factors describing the shift in the allosteric equilibrium constants were determined experimentally and are therefore independent of the modulator-binding model. According to the nested MWC model at pH 7.55, conformation tT prevails with at least 98% at 1 Torr and conformation rT prevails with at least 98% at 150 Torr. This is the case irrespective of the presence or absence of urate and caffeine. Thus, at pH 7.55, it can be concluded that under normoxic conditions the binding constant u_{rT} for conformation rT and under hypoxic conditions the binding constant u_{tT} for conformation tT are measured. Thus, the value for $F_{T,u}$ as obtained from the affinities can be compared to the experimentally determined value to test the model.

The binding constant for urate observed under hypoxic conditions is $u_{tT} \approx 4\ mM^{-1}$ and at 150 Torr oxygen pO_2 $u_{rT} \approx 8.5\ mM^{-1}$. Thus, the predicted value for $F_{T,u}$ is 0.56, which obviously does not agree with the results of the analysis of the oxygen-binding curves showing a $F_{T,u} = 0.043$. The same conclusion follows from an inspection of the results for the three-state model: here, the corresponding factor is $W_{T,u} = 0.036$ with the hexamer as the allosteric unit, which is also far off from 0.56. For the three-state model with the dodecamer as the allosteric unit, the experimentally determined value is $W_{T,u} = 0.0021$ and the predicted value is $0.56^2 = 0.31$. Actually, the differences in the affinity constants u_{tT} and u_{rT} are so small (just a factor of 2) that they would not lead to a significant change in conformational distribution for any allosteric model. Thus, an alternative model for the interpretation of the calorimetric data is needed.

To account for the low value of $F_{T,u}$ with only one binding site per hexamer, either a much higher binding constant for conformation rT or a much lower binding constant for tT is needed. Possibly, binding to the allosteric binding site of a hexamer in conformation tT occurs with a very low, nondetectable affinity, and the binding process actually observed under hypoxic conditions is an unrelated process like binding to a nonallosteric site with a binding affinity $K_{nonallo}$. Indeed, such a model is in good agreement with the whole set of data. If we assume that the affinity constant of $4\ mM^{-1}$ reflects urate binding to a nonallosteric site, then the highest affinity of conformation tT, which is in agreement with the urate-binding data in the absence of oxygen, amounts to $u_{tT} \approx 0.5\ mM^{-1}$. The binding curve obtained under normoxic conditions contains modulator binding to the nonallosteric sites plus allosteric binding to conformation rT. Unfortunately, the rather low overall affinity of urate did not allow determining the binding affinities just based on the calorimetric data. Thus, u_{rT} was calculated based on $F_{T,u} = 0.043 = [(1 + 0.5)/(1 + u_{rT})]$, yielding a value of $u_{rT} = 34\ mM^{-1}$. With $K_1 = u_{rT} = 34\ mM^{-1}$ and $K_2 = K_{nonallo} = 4\ mM^{-1}$ held constant, the binding enthalpies could be derived from fitting a model of two types of sites to the urate-binding curve in the absence of oxygen.

In contrast, the caffeine-binding curve at pH 7.55 in the presence of oxygen could be analyzed based on two types of sites without any preset value for the affinities. Then, binding to the nonallosteric site occurs with an affinity of $33 \pm 2\ mM^{-1}$ and binding to conformation rT with $c_{rT} = 361 \pm 48\ mM^{-1}$. On the basis of the factor $F_{T,c} = 0.0065 = (1 + c_{tT})/(1 + 361)$ the affinity for conformation tT ($c_{tT} = 1.3\ mM^{-1}$) could be determined. Binding of caffeine in the absence of oxygen was then reanalyzed based on a model of two types of sites with $K_1 = c_{tT} = 1.3\ mM^{-1}$ and $K_2 = K_{nonallo} = 33\ mM^{-1}$, yielding the corresponding binding enthalpies.

The binding constants of urate and caffeine for conformation rR and tR can be calculated based on F_u, $F_{R,u}$ and F_c, $F_{R,c}$, respectively. The binding affinities and enthalpies are summarized in Table 4. The resulting calculated curves are shown together with the fits based on the previous, simpler models. In each case, the curves based on a model of two types of two sites per dodecamer yielded an equally good fit as the model based on two sites per dodecamer (Figure 3). Thus, on the basis of the data obtained at pH 7.55, a general model describing both effector binding and oxygen-binding data was found.

DISCUSSION

Crustacean hemocyanins are highly cooperative and allosterically regulated proteins that bind oxygen at the gills and transport it to the tissues where oxygen is released (*2*, *39*,

40). This Janus-faced efficient uptake and delivery of oxygen by the respiratory pigment is modulated by various effectors. Whereas protons decrease oxygen affinity, all physiological compounds such as inorganic ions, neurohormones, and the metabolites L-lactate and urate increase oxygen affinity (*5*).

Urate is of particular interest because it is a common metabolite of crustaceans resulting from nucleotide degradation. During hypoxia, this purine derivative increases its concentration about 10-fold in the hemolymph, because in the animal tissues, the pO_2 is too low to saturate uricase with oxygen, thus diminishing the enzymes activity (*41*). Urate (1 mM) causes a pH-dependent shift of the p50 to values that are about 50−60% lower than those without the modulator. In addition, urate diminishes cooperativity slightly as indicated by a decrease of the Hill coefficients from an average of 4.0 to 3.4. This modulation of oxygen affinity is even more pronounced in the presence of the nonphysiological purine derivative caffeine.

Employing ITC, the binding behavior of urate and caffeine to hemocyanin under normoxic conditions was previously reported (*31*). Under these conditions, urate binds noncooperatively to two identical binding sites with an pH-independent microscopic affinity constant of about 8.5 mM^{-1}, whereas caffeine binds cooperatively with $K_1 = 14\ mM^{-1}$ and $K_2 = 40-70\ mM^{-1}$, irrespective of pH. In contrast, ITC-binding experiments under hypoxic conditions show decreased affinities for urate and caffeine (Table 3).

The mechanism by which urate modulates the oxygen-binding properties is not known, and until now, no attempt has been made to characterize the binding properties of hemocyanin from *H. vulgaris* in terms of a cooperative model. To understand the mechanism of allosteric interaction between binding of oxygen, urate, caffeine, and protons to this hemocyanin, we tried to establish a cooperative model that can account for the modulation of hemocyanin oxygen affinity by these compounds.

Urate and caffeine increase the average oxygen affinity of hemocyanin from *H. vulgaris*, indicating that both modulators bind more strongly to the oxygenated form than to the deoxygenated form. This interpretation is corroborated by ITC-binding experiments, which showed a decreased value for the microscopic binding constants for urate and caffeine under hypoxic conditions (Table 3). For a quantitative comparison, the respective binding stoichiometry and binding affinities are needed. The number of binding sites for urate cannot be determined from the calorimetric data under normoxic conditions, because the protein concentration of hemocyanin could not be raised to such an extent that a sufficiently high value of the product of K, n, and [Hc] would result. Therefore, for the interpretation of the binding data, the number of binding sites for urate was set to $n = 2$ per dodecamer, which is in accordance with the results obtained previously from equilibrium dialysis (*15*). With regard to caffeine, however, the analysis of binding isotherms under normoxic conditions using a "multiple-noninteracting-site model" resulted in three binding sites, which cannot be easily explained in view of the quaternary structure of the pigment and of a putative location of the binding sites. Furthermore, one would expect the same number of binding sites as found for urate. However, binding of caffeine could also be explained based on a "cooperative binding model" with two interacting binding sites (*31*). The latter interpretation is supported by the fact that in the analysis of caffeine binding to deoxygenated hemocyanin two binding sites were obtained if identical noninteracting binding sites were assumed. Thus, two binding sites per dodecameric hemocyanin molecule are in accordance with all studies where binding of the modulators caffeine and urate were investigated.

To establish a model that can account for the regulation of oxygen uptake and release of the hemocyanin of *H. vulgaris* by protons and urate, we tried to combine the results obtained from modulator binding studies with results from the analysis of oxygen-binding curves in the absence and presence of the modulator. The cooperative oxygen binding of a number of hemocyanins is well-explained in terms of concerted models such as the MWC, three-state, or nested MWC models (*7*, *21*, *24*, *25*, *27*, *37*, *38*). A feature in common with all concerted models is that different conformations are postulated, which are characterized by their specific ligand and modulator-binding constants (*42*). The presence of a ligand or a modulator induces a shift in the conformational distributions of the protein. The 2×6-meric hemocyanin from *H. americanus* may serve as a typical example. It was shown that the pH value only influences the value of the allosteric equilibrium constants in the framework of the nested MWC model, while the oxygen-binding constants for the four conformations are independent of pH, ranging from 7.0 to 8.2 (*38*). Thus, the allosteric equilibrium constants as obtained from the analysis of ligand-binding curves are a function of the modulator concentration (eqs 3 and 5). The exact form of this function depends on the model assumed for modulator binding.

In this study, we show that oxygen-binding data for hemocyanin of the closely related lobster *H. vulgaris* can also be well-described by the nested MWC model. The nested MWC model yielded a better agreement between data and fit than the three-state MWC model (Table 2). However, the three-state MWC model cannot be ruled out completely. In any case, the oxygen-binding behavior can be explained in very good agreement with the data based on a concerted model (three-state or nested MWC models) in which the hexamers form the allosteric unit that can adopt different conformations. To understand the allosteric regulation of this hemocyanin, a binding model for the modulators urate and caffeine also has to be postulated. Thus, we have to find the number of binding sites per allosteric unit and the affinities of the modulators for the different conformations available for the allosteric unit. The model for modulator binding has to be in agreement with the binding curves obtained for the modulator and be able to explain the observed shift in the allosteric equilibrium constants because of the presence of the modulator.

The simplest modulator-binding model failed to account for the observed shift in the allosteric equilibrium constants. The calorimetrically obtained affinity constants of the modulators determined under normoxic and hypoxic conditions differ only by about a factor of 2 (for urate) or maximally 4 (for caffeine). This means that, for urate at a stoichiometry of 2, as proposed by the most simple model, the equilibrium constant between the conformation present under normoxic and hypoxic conditions is shifted by a factor of about $2^2 = 4$ at most (at sufficiently high concentrations). However, the conformational equilibrium constants for both the nested MWC model and the three-state model are shifted

largely. Thus, either the difference between the affinities is underestimated or the stoichiometry is much higher than assumed so far. Because the stoichiometry of 2 is confirmed by two different methods (*15*, *16*, *31*), the interpretation of the binding constants for urate as determined in the calorimetric experiments was reconsidered to explain the discrepancies. In the calorimetric experiment, every modulator-binding event is contributing to the binding curve whether binding is connected to allosteric regulation or not. In contrast, in the oxygen-binding curves, only the allosteric binding sites contribute to the shift in the conformational distribution. Indeed, it is possible to find a set of binding affinities for two allosteric and two nonallosteric binding sites per 2× hexamer that are in full agreement with the observed shift in the conformational distribution in the oxygen-binding experiments and the observed binding curves in the calorimetric experiments. Alternatively, one could speculate that the binding affinity as found under hypoxic conditions is too high because the oxygen concentration was in fact higher than intended. We dismiss this explanation because the actual oxygen concentration in the glovebox was monitored continuously and did not exceed 1 Torr.

Another puzzling result was the absence of any pH dependence in the calorimetrically obtained affinities for urate and caffeine both under normoxic and hypoxic conditions. At first glance, this finding seems to contradict the predictions made based on the oxygen-binding data, which showed that the shift in the p50 values is pH-dependent. This in fact means that the presence of protons, which act as an inhibitor, shifts the conformational distribution in the opposite direction from the modulator urate or caffeine. However, a significant effect on the affinity of the modulator under normoxic or hypoxic conditions can only be expected if the protons shift the conformational distributions under these conditions to a significant extent. For hypoxic conditions, the absence of any pH dependence can be explained easily by the presence of nonallosteric binding sites. As pointed out above, under hypoxic conditions, the binding curve is predominantly governed by binding to the nonallosteric sites, because binding to the allosteric sites occurs with a much lower affinity and does not contribute significantly to the measured binding enthalpy. These nonallosteric binding sites are not necessarily pH-dependent because their affinity does not depend on the conformation. However, for the binding of modulators to the oxygenated state, this reasoning does not apply, because the observed binding process is governed by binding to the allosteric sites also.

Thus, we calculated the conformational distributions at 150 Torr for the modulator concentrations in the titration experiments based on the nested MWC model with the affinities as given in Table 3. Then, effector-binding curves at different pH values were simulated based on these conformational distributions. The results for pH 7.85 and 8.15 are depicted in Figure 4. For practical reasons, the curves are depicted as binding curves and not as differential binding curves as measured in the ITC experiments. The simulated curves for caffeine do not differ much for the two pH values in the oxygenated state (Figure 4).

Further support for our model of modulator binding to allosteric and nonallosteric sites is found in an earlier report on urate binding. Zeis et al. (*16*) observed some "unspecific" binding in dialysis experiments for urate binding at pH 8.0 and 15 °C under normoxic conditions, leading to a stoichiometry of about 3 urate molecules per dodecamer. The binding curves as simulated for urate under normoxic conditions based on our model are qualitatively in agreement with this observation (Figure 4).

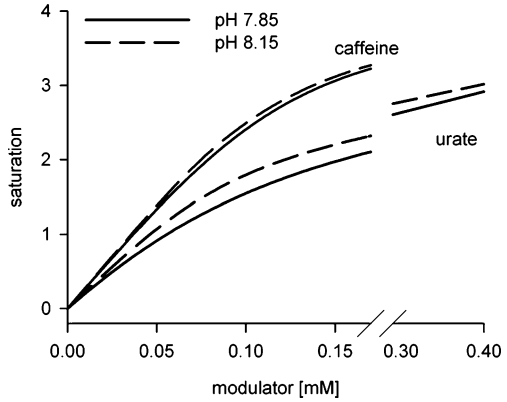

FIGURE 4: Simulation of urate- and caffeine-binding curves under concentrations as used in the ITC experiments. On the basis of the binding parameters and allosteric equilibrium constants as determined for the nested MWC model, binding curves were simulated for the experimental conditions as used in the ITC experiments under normoxic conditions (35 μM hemocyanin and 0.15 mM caffeine) for two pH values 8.15 and 7.85.

The model for modulator binding presented here is the simplest model in agreement with calorimetric modulator-binding data and the shift of conformational distributions because of the modulator as deduced from the analysis of oxygen-binding curves. In this model, two allosteric and two nonallosteric urate/caffeine-binding sites per dodecamer exist. On the basis of the structure of this hemocyanin, the position of these binding sites is not evident. Rather, one would expect four binding sites, which are located at the vertexes of the trimer and are all allosterically active. A model assuming two allosteric binding sites per hexamer with different affinities would meet this requirement. However, in such a model, the number of binding constants (for each conformation, two types, giving a total of eight) is too large to be distinguishable based on the present data. The presence of nonallosteric urate-binding sites was also postulated for another hemocyanin, the 2 × 6-mer from *Astacus leptodactylus* (*43*). However, the stoichiometry of binding was four nonallosteric and four allosteric binding sites per dodecamer. Here, the information about the quaternary structure (also a 2× hexamer) supports this interpretation.

Physiological Considerations. The results obtained in this study are well-suited to gain deeper insights in the role of urate under different physiological conditions, such as at rest and under environmental and functional hypoxia. Under normoxic conditions, the pO_2 in the hemolymph of *H. vulgaris* is about 21 Torr when arriving at the gills and about 50 Torr after gill passage (*44*). The pH was found to be around 8.0 (*45*, *46*). On the basis of the oxygen-binding curves shown in Figure 5 for these conditions, the affinity of the pigment is so high that only a fraction (maximum of 15%) of the bound oxygen is unloaded at the tissues. Most of the utilized oxygen is therefore physically dissolved and not delivered by the respiratory pigment.

Under moderate environmental hypoxia, the concentrations of positive heterotropic modulators such as L-lactate and urate increase in the hemolymph of some crustaceans (*13*, *18*, *44*,

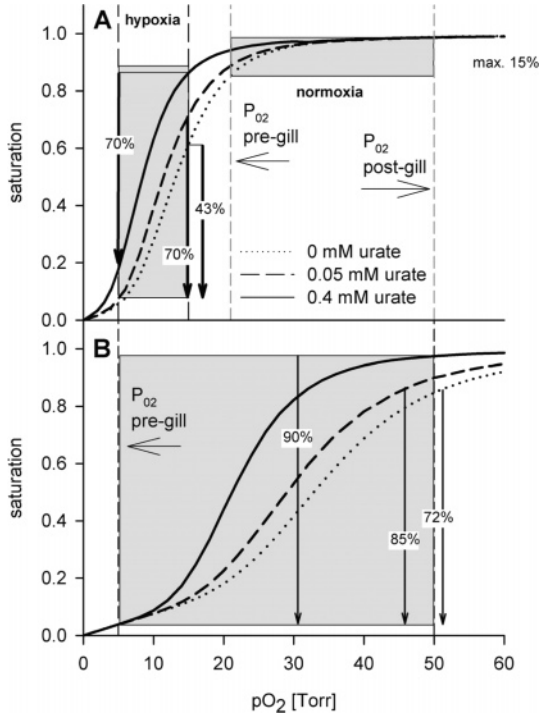

FIGURE 5: Simulated *in vivo* oxygen-binding curves for hemocyanin of the European lobster (*H. vulgaris*). Oxygen-binding behavior of hemocyanin was simulated for different conditions such as environmental (A, pH 8.0) and functional (B, pH 7.55) hypoxia. Vertical broken lines indicate the oxygen partial pressure before and after the gills. The three binding curves shown in each panel are simulated binding curves for a total concentration of 0, 50, and 400 μM urate at a hemocyanin concentration of 35 μM. (A) Under normoxic conditions, the pH of the hemolymph is 8.0 and the partial pressure before and after passage through the gills is 21 and 50 Torr (gray broken lines). The transport capacity with or without urate is rather small, at most 15%. Under environmental hypoxia, the oxygen pressure at the gills drops to 15 and 5 Torr at the tissue (black broken lines). Without urate, the transport capacity corresponds to 43% unloading of hemocyanin at the tissue, in the presence of 50 or 400 μM urate and the capacity increases to about 70%. (B) Under functional hypoxia, the oxygen pressure at the tissue drops to about 5 Torr and the pH to about 7.5. At this pH, the saturation level of hemocyanin at 5% Torr does not depend on the urate concentration. The increase of oxygen capacity is caused by an increased level of saturation at the gills at 50 Torr because of the presence of urate, increasing the capacity from 72% (no urate) to 85% (50 μM urate) and 90% (400 μM urate).

47−*49*). Typical values for urate are 50 μM under normoxic conditions and 400 μM under hypoxic conditions (*18*). Furthermore, the pO_2 in the hemolymph decreases prebranchially to ∼4−8 Torr and to approximately 15 Torr (*45*, *46*) after passing the gills. However, no significant change in the hemolymph pH was found (*44*−*46*). Under these conditions, the fraction of oxygen delivered to the tissues would be about 43% in the absence of urate (nonphysiological) and would increase to about 70% in the presence of urate (Figure 5). However, the effect on oxygen deliverance is not significantly different in the presence of 50 or 400 μM urate. Thus, for moderate environmental hypoxia, the increase in the urate concentration from 50 to 400 μM does not change the transport capacity. However, a concentration of 50 μM urate seems to be sufficient to maximize oxygen delivery compared to the absence of the natural modulator urate.

Functional hypoxia caused by elevated muscular activity is characterized by an increased oxygen demand at a constant environmental oxygen supply and accompanied by hemolymph acidification. A decrease of hemolymph pH from 8.0 to 7.55 was found in the closely related *H. americanus* (*50*). Under these conditions, urate compensates for the proton-induced decrease in oxygen saturation at the gills (Figure 5b) and enhances oxygen loading of hemocyanin. It seems that the physiological role of urate is to compensate the effects of stressful conditions on the oxygen-binding properties of hemocyanin during elevated locomotory activity, especially if environmental hypoxia also exists.

The present effector binding studies support the applicability of concerted models such as the MWC model or the nested MWC model to the modulation of oxygen transport in hemocyanins. Furthermore, this study demonstrates the importance of combining ligand- and effector-binding data to obtain reliable models for effector binding. The strategy presented here is applicable to any macromolecular system that can be described by a subset of conformations that are shifted in their equilibrium by the presence of effectors and ligands. Thus, the analytical procedure is of general relevance for this type of allosteric and cooperative regulation.

The MWC model describes well the oxygen-binding properties of hemocyanin from *A. leptodactylus* (*51*), whereas for the hemocyanin from *H. vulgaris*, a more complex model such as the nested MWC model has to be assumed. In both cases, a complex binding behavior for the modulators urate and caffeine have to be postulated, possibly involving nonallosteric binding sites. In addition, it is remarkable that the respiratory pigment only transports a significant amount of oxygen during physiological stressful situations such as enhanced locomotory activity corroborating earlier studies on the role of hemocyanin in the shore crab *Carcinus maenas* and in the tarantula *E. californicum* that led to the same conclusion (*52*).

REFERENCES

1. Markl, J., and Decker, H. (1992) Molecular structure of arthropod hemocyanins, *Adv. Comput. Environ. Physiol. 13*, 325−376.
2. van Holde, K. E., and Miller, K. I. (1982) Haemocyanins, *Q. Rev. Biophys. 15*, 1−129.
3. van Holde, K. E., and Miller, K. I. (1995) Hemocyanins, *Adv. Protein Chem. 47*, 1−81.
4. van Holde, K. E., Miller, K. I., and van Olden, E. (2000) Allostery in very large molecular assemblies, *Biophys. Chem. 86*, 165−172.
5. Bridges, C. R. (2001) Modulation of haemocyanin oxygen affinity: Properties and physiological implications in a changing world, *J. Exp. Biol. 204*, 1021−1032.
6. Truchot, J. P. (1975) Factors controlling the *in vitro* and *in vivo* oxygen affinity of the hemocyanin in the crab *Carcinus maenas* (L.), *Respir. Physiol. 24*, 173−189.
7. Brouwer, M., and Serigstad, B. (1989) Allosteric control in *Limulus polyphemus* hemocyanin: Functional relevance of interactions between hexamers, *Biochemistry 28*, 8819−8827.
8. Brouwer, M., Bonaventura, C., and Bonaventura, J. (1978) Analysis of the effect of three different allosteric ligands on oxygen binding by hemocyanin of the shrimp, *Penaeus setiferus*, *Biochemistry 17*, 2148−2154.
9. Sanders, N. K., and Childress, J. J. (1992) Specific effects of thiosulfate and L-lactate on hemocyanin−O_2 affinity in brachyuran hydrothermal vent crab, *Mar. Biol. 113*, 175−180.
10. Taylor, A. C., Johns, A. R., Atkinson, R. J. A., and Bridges, C. R. (1999) Effects of sulphide and thiosulphate on the respiratory properties of haemocyanin of the benthic crustaceans *Caloricaris macandreae* Bell, *Nephrops norvegicus* (L.), and *Carcinus maenas* (L.), *J. Exp. Mar. Biol. Ecol. 233*, 163−179.

11. Morris, S., and McMahon, B. R. (1989) Potentiation of hemocyanin oxygen affinity by catecholamines in the crab cancer magister: A specific effect of dopamine, *Physiol. Zool. 62*, 654−667.
12. McMahon, B., and Morris, S. (1990) Neurohormonal and metabolic effects on oxygen binding by crustacean hemocyanin, in *Invertebrate Oxygen Carriers* (Préaux, G., and Lontie, R., Eds.) pp 461−465, Leuven Press, Belgium, Germany.
13. Truchot, J. P. (1980) Lactate increases the oxygen affinity of crab hemocyanin, *J. Exp. Zool. 214*, 205−208.
14. Hartmann, H., Lohkamp, B., Hellmann, N., and Decker, H. (2001) The allosteric effector L-lactate induces a conformational change of 2 × 6-meric lobster hemocyanin in the oxy state as revealed by small-angle X-ray scattering, *J. Biol. Chem. 276*, 19954−19958.
15. Zeis, B., Nies, A., Bridges, C. R., and Grieshaber, M. K. (1992) Allosteric modulation of haemocyanin oxygen-affinity by L-lactate and urate in the lobster *Homarus vulgaris*. I. Specific and additive effects on haemocyanin oxygen-affinity, *J. Exp. Biol. 168*, 93−110.
16. Nies, A., Zeis, B., Bridges, C. R., and Grieshaber, M. K. (1992) Allosteric modulation of haemocyanin oxygen-affinity by L-lactate and urate in the lobster *Homarus vulgaris*. II. Characterization of specific effector binding sites, *J. Exp. Biol. 168*, 111−124.
17. Morris, S., Bridges, C. R., and Grieshaber, M. K. (1985) A new role for uric acid: Modulator of haemocyanin affinity in crustaceans, *J. Exp. Zool. 235*, 135−139.
18. Czytrich, H. M., Bridges, C. R., and Grieshaber, M. (1987) Purinstoffwechsel von *Astacus leptodactylus*, *Verh. Dtsch. Zool. Ges. 80*, 207.
19. Lallier, F., Boitel, F., and Truchot, J. P. (1987) The effect of ambient oxygen and temperature on haemolymph L-lactate and urate concentration in the shore crab *Carcinus maenas*, *Comp. Biochem. Physiol. A: Mol. Integr. Physiol. 86*, 255−260.
20. Morris, S., Bridges, C. R., and Grieshaber, M. K. (1986) The potentiating effect of purine bases and some of their derivatives on the oxygen affinity of haemocyanin from the crayfish *Austropotamobius* pallipedes, *J. Comput. Physiol. B 156*, 431−440.
21. Decker, H., Connelly, P. R., Robert, C. H., and Gill, S. J. (1988) Nested allosteric interaction in tarantula hemocyanin revealed through the binding of oxygen and carbon monoxide, *Biochemistry 27*, 6901−6908.
22. Hellmann, N., Raithel, K., and Decker, H. (2003) A potential role for water in the modulation of oxygen binding by tarantula hemocyanin, *Comp. Biochem. Physiol. A: Mol. Integr. Physiol. 136*, 725−734.
23. Sterner, R., Bardehle, K., Paul, R., and Decker, H. (1994) Tris: An allosteric effector of tarantula haemocyanin, *FEBS Lett. 339*, 37−39.
24. Dainese, E., Di Muro, P., Beltramini, M., Salvato, B., and Decker, H. (1998) Subunits composition and allosteric control in *Carcinus aestuarii* hemocyanin, *Eur. J. Biochem. 256*, 350−358.
25. Johnson, B. A., Bonaventura, C., and Bonaventura, J. (1988) Allostery in *Callinectes sapidus* hemocyanin: Cooperative oxygen binding and interactions with L-lactate, calcium, and protons, *Biochemistry 27*, 1995−2001.
26. Makino, N. (1987) The oxygenation-linked binding of neutral red to spiny lobster hemocyanin. A structural study of the partially oxygenated protein, *Eur. J. Biochem. 163*, 35−41.
27. Arisaka, F., and van Holde, K. E. (1979) Allosteric properties and the association equilibria of hemocyanin from *Callianassa californiensis*, *J. Mol. Biol. 134*, 41−73.
28. Hellmann, N. (2004) Bohr-effect and buffering capacity of hemocyanin from the tarantula *E. californicum*, *Biophys. Chem. 109*, 157−167.
29. Sick, H., and Gersonde, K. (1969) Method for continuous registration of O_2-binding curves of hemoproteins by means of a diffusion chamber, *Anal. Biochem. 32*, 362−376.
30. Bridges, C. R., Bicudo, J. E. P. W., and Lykkeboe, G. (1979) Oxygen content measurements in blood containing hemocyanine, *Comp. Biochem. Physiol., Part A: Mol. Integr. Physiol. 62*, 457−462.
31. Menze, M. A., Hellmann, N., Decker, H., and Grieshaber, M. K. (2000) Binding of urate and caffeine to hemocyanin of the lobster *Homarus vulgaris* (E.) as studied by isothermal titration calorimetry, *Biochemistry 39*, 10806−10811.
32. Wiseman, T., Williston, S., Brandts, J. F., and Lin, L. N. (1989) Rapid measurement of binding constants and heats of binding using a new titration calorimeter, *Anal. Biochem. 179*, 131−137.
33. Scheibe, P., Bernt, E., and Bergmeyer, H. U. (1974) *Methoden der Enzymatischen Analyse* (Bergmeyer, H. U., Ed.) pp 1999−2002, Verlag Chemie, Weinheim, Germany.
34. Minton, A. P., and Imai, K. (1974) The three-state model: A minimal allosteric description of homotropic and heterotropic effects in the binding of ligands to hemoglobin, *Proc. Natl. Acad. Sci. U.S.A. 71*, 1418−1421.
35. Robert, C. H., Decker, H., Richey, B., Gill, S. J., and Wyman, J. (1987) Nesting: Hierarchies of allosteric interactions, *Proc. Natl. Acad. Sci. U.S.A. 84*, 1891−1895.
36. Monod, J., Wyman, J., and Changeux, J. P. (1965) On the nature of allosteric transitions: A plausible model, *J. Mol. Biol. 12*, 88−118.
37. Connelly, P. R., Johnson, C. R., Robert, C. H., Bak, H. J., and Gill, S. J. (1989) Binding of oxygen and carbon monoxide to the hemocyanin from the spiny lobster, *J. Mol. Biol. 207*, 829−832.
38. Decker, H., and Sterner, R. (1990) Nested allostery of arthropodan hemocyanin (*Eurypelma californicum* and *Homarus americanus*). The role of protons, *J. Mol. Biol. 211*, 281−293.
39. Ellerton, H. D., Ellerton, N. F., and Robinson, H. A. (1983) Hemocyanin−A current perspective, *Prog. Biophys. Mol. Biol. 41*, 143−248.
40. van Holde, K. E., Miller, K. I., and Decker, H. (2001) Hemocyanins and invertebrate evolution, *J. Biol. Chem. 276*, 15563−15566.
41. Dyken, J. A. (1991) Purineolytic capacity and origin of hemolymph urate in *Carcinus maenas* during hypoxia, *Comp. Biochem. Physiol., Part B: Biochem. Mol. Biol. 98*, 579−582.
42. Wyman, J., and Gill, S. J. (1990) *Binding and Linkage*, University Science Books, Herndon, VA.
43. Hellmann, N., Jaenicke, E., and Decker, H. (2001) Two types of urate binding sites on hemocyanin from the crayfish *Astacus leptodactylus*: An ITC study, *Biophys. Chem. 90*, 279−299.
44. Lallier, F., and Truchot, J. P. (1989) Hemolymph oxygen transport during environmental hypoxia in the shore crab, *Carcinus maenas*, *Respir. Physiol. 77*, 323−336.
45. Butler, P. J., Taylor, E. W., and McMahon, B. R. (1978) Respiratory and circulatory changes in the lobster (*Homarus vulgaris*) during long-term exposure to moderate hypoxia, *J. Exp. Biol. 73*, 131−146.
46. McMahon, B. R., Butler, P. J., and Taylor, E. W. (1978) Acid−base changes during recovery from disturbance and during long-term hypoxic exposure in the lobster *Homarus vulgaris*, *J. Exp. Biol. 205*, 361−370.
47. Johnston, W., Bonaventura, C., and Bonaventura, J. (1984) Allosteric modulation of *Callinectes sapidus* hemocyanin by binding of L-lactate, *Biochemistry 23*, 872−878.
48. Bouchet, J. Y., and Truchot, J. P. (1984) Effects of hypoxia and L-lactate on the haemocyanin−oxygen affinity of the lobster, *Homarus vulgaris*, *Comp. Biochem. Physiol., Part A: Mol. Integr. Physiol. 80*, 69−73.
49. Lallier, F., and Truchot, J. P. (1989) Hemolymph oxygen transport during environmental hypoxia in the shore crab, *Carcinus meanas*, *Respir. Physiol. 77*, 323−336.
50. Rose, R. A., Wilkens, J. L., and Walker, R. L. (1998) The effects of walking on heart rate, ventilation rate, and acid-based status in the lobster *Homarus americanus*, *J. Exp. Biol. 201*, 2601−2608.
51. Hellmann, N., Hörnemann, J., Jaenicke, E., and Decker, H. (2003) Urate as effector for crustacean hemocyanins, *Micron 35*, 109−110.
52. Paul, R., Bergner, B., Pfeffer-Seidl, A., Decker, H., Efinger, R., and Storz, H. (1994) Gas transport in the haemolymph of arachnids−Oxygen transport and the physiological role of haemocyanin, *J. Exp. Biol. 188*, 25−46.

BI050507S